



## Effects of Hydrogen-Addition on a Bio-fueled SI Engine Performance, Fuel Consumption and Greenhouse Gas Emissions

Ali Qasemian<sup>1\*</sup>, Sina Jenabi Haghparast<sup>2</sup>, Pouria Azarikhah<sup>3</sup>

<sup>1</sup> Assistant professor, School of Automotive Engineering, Iran University of Science and Technology, Tehran, Iran

<sup>2</sup> M. Sc., School of Automotive Engineering, Iran University of Science and Technology, Tehran, Iran

<sup>3</sup> M. Sc., Department of Mechanical Engineering, Iran University of Science and Technology, Tehran, Iran

### ARTICLE INFO

#### Article history:

Received: 12 Nov 2022

Accepted: 14 Nov 2022

Published: 14 Nov 2022

#### Keywords:

SI engine

Bio-fuel

Ethanol

Hydrogen

GHG Emissions

### ABSTRACT

In the current study, the hydrogen-addition influence on the performance of an SI engine using a gasoline-ethanol blend is investigated numerically. The simulation and validation of the model are carried out in order to evaluate the engine performance using conventional gasoline (G100) and the blend of gasoline and ethanol (G75E25). Furthermore, the hydrogen is added to the gasoline-ethanol blend (G50E25H25) to improve the engine thermal efficiency and reduce the amount of brake specific fuel consumption (BSFC) which leads to the reduction in greenhouse gas (GHG) emissions. The brake specific carbon dioxide (BSCO<sub>2</sub>) is also studied in this paper. Results show that the addition of hydrogen increases the brake power and thermal efficiency, moderates the BSFC, and decreases the maximum temperature of combustion chamber which reduces the production of greenhouse gases as well as BSCO<sub>2</sub>. In comparison with pure gasoline, by using G50E25H25, the maximum temperature of in-cylinder gas decreased by 12.55%, 10.82%, and 13.43% at 2000, 4000, and 6000 rpm, respectively. It is also evaluated that the lowest amount of BSCO<sub>2</sub> is related to G50E25H25 in most of the engine speeds. The bio-fuel of G75E25 and pure gasoline are placed in next positions, respectively.

\*Corresponding Author

Email Address: [Qasemian@iust.ac.ir](mailto:Qasemian@iust.ac.ir)

<https://doi.org/10.22068/ase.2022.619>

## 1. Introduction

Despite the fact that global fossil energy resources are coming to an end, petroleum resources play a significant role in automotive industry, which can result in environmental problems such as global warming and air pollution [1-5]. During previous years, different methods and techniques such as vehicle electrification and using bio alternative fuels have been applied to conventional vehicles to reduce the mentioned crises of fossil fuels [6-10]. In the case of utilizing alternative bio-fuels, many researchers have investigated the effects of different bio-fuels such as methanol, ethanol, and n-butanol on engine efficiency [11-13], emission characteristics [14-16], knock probability [17-20], and fuel consumption [21-23] of spark ignition and compression ignition engines.

Jeevahan et al. [24] studied the effects of 1-butanol/biodiesel blends on the engine performance and emissions characteristics of a single-cylinder compression ignition engine. They concluded that the addition of 1-butanol slightly reduces the brake thermal efficiency as compared to that of neat biodiesel. However, there is a reduction in specific fuel consumption, exhaust gas temperature and emissions of tested gases including NO<sub>x</sub>, CO and HC.

Gupta and Mittal [25] performed a comparative study on a spark-ignition engine operated with gasoline and methane in different load conditions. This comparative investigation indicated that the BSFC of the engine using methane was lower compared to conventional gasoline at all engine loads. However, the combustion duration was longer for methane as compared to gasoline. The emission of nitrogen oxide decreased for methane, with a reduction of about 22% at higher load of 14 N.m. Furthermore, the emission of hydrocarbon was also reduced for methane, with a reduction of about 51% at 14 N.m. Also, the decrement of CO and CO<sub>2</sub> emissions were noticeable in engine consuming methane.

Nayyar et al. [26] studied the performance and emissions of oxygenated ternary fuel mixtures to specify the optimum ratio of blends in aspect of emissions reduction. The nitromethane-n-butanol–diesel blend is termed as bio-oxygenated fuel. Baseline data were generated by using diesel and a blend of 20%

(v/v) n-butanol with diesel (B20). Their results showed that the optimum emissions reduction was related to 1% of nitromethane by volume (NM1B20). They realized that nitromethane-n-butanol–diesel blends are highly efficient alternatives to reduce emissions in compression ignition engines with a slight improvement in performance characteristics.

Galloni et al. [27] analyzed the behavior of various blends of alcohol and gasoline in a downsized SI engine. At low load, the optimum spark advance is not more sensitive to the fuel composition. Increasing the alcohol percentage in the mixture, the spark advance can be reduced due to the higher alcohol flame speed compared to that of pure gasoline. At high load, the spark advance is knock limited. Due to the alcohol higher knock resistance, with respect to gasoline, the spark time can be advanced. So the fuel conversion efficiency may benefit from this new engine setting.

Natarajan et al. [28] experimentally analyzed the early direct injection in an HCCI engine. In order to conduct investigation, the neat diesel and bio ethanol-diesel blend (E20) were used as fuel and the pressure, combustion and emission characteristics were studied in the equivalence ratio of 0.6. The injection timing was advanced to 18° rather than the normal 23° BTDC. They showed that the major emission of an HCCI engine is unburned hydrocarbons. In general, HC emission is produced due to the incomplete combustion which is caused due to the insufficient oxygen available for combustion. They concluded that the emission of unburned hydrocarbons reduced by about 9% when bio ethanol-diesel blend (E20) is used as fuel.

Regarding the previous studies, the effects of hydrogen-addition on the performance and emissions of bio-fueled spark ignition engines are not considered noticeably by former investigators. In the first step of this study, the volumetric mixture of 75% pure gasoline and 25% ethanol (G75E25) is used to gain advantages of alcoholic fuels characteristics. In the next step, the volume of 25% hydrogen is added to the mentioned blend in order to improve the thermal efficiency and the brake specific fuel consumption (BSFC). Moreover, the influence of hydrogen-addition on the maximum gas temperature in combustion chamber and brake specific carbon dioxide (BSCO<sub>2</sub>) will be also examined. Therefore, a

new gasoline-ethanol-hydrogen fuel blend (G50E25H25) will be introduced and investigated numerically for comparison of the mentioned characteristics with G100 and G75E25. As an alternative fuel, G50E25H25 is a volumetric blend of 50% gasoline, 25% ethanol, and 25% hydrogen.

## 2. Numerical Modelling

The engine is considered as a closed thermodynamic system and differential energy equation is used in order to analyze the energy balance of the engine. The differential energy balance is utilized for small variations of crank angle.

The required information for simulation including engine geometry, AF ratio, and valves lift, etc. are provided from experimental data. The parameter of  $P-\theta$  is achieved by the implicit differential equation of in-cylinder pressure. The implicit ODE is shown in Eq. (1) which will be solved through forth order Runge-Kutta technique. The three parameters of  $\frac{dV}{d\theta}$ ,  $\frac{dx_b}{d\theta}$  and  $\frac{dq_w}{d\theta}$  are calculated via sub-models which will be introduced in next parts.

$$\frac{dP}{d\theta} = -\gamma \frac{P}{V} \frac{dV}{d\theta} + \frac{\gamma - 1}{V} (q_{in} \frac{dx_b}{d\theta} - \frac{dq_w}{d\theta}) \quad (1)$$

### 2.1. Engine Geometry

The technical specifications of the studied engine are illustrated in Table 1. The volume of the single-cylinder, four-stroke, and SI engine is 124.1 cc and the compression ratio of the engine is 9.1.

**Table 1:** Technical specifications of the single-cylinder engine

Volume (cc)	124.1
Bore (mm)	56.5
Stroke (mm)	49.5
Arrangement of Valves	Two OHC valves
Compression ratio	9.1:1
Rated power (hp)	9.92 (8492 rpm)
Rated torque (N.m)	9.23 (6997 rpm)
Intake valve timing	5° bTDC/35° aBDC
Exhaust valve timing	30° bBDC/5° aTDC

In order to calculate cylinder volume in every crank angle ( $\theta$ ), Eq. (2) is considered.

$$V = V_c + \frac{\pi B^2}{4} (l + r - s) \quad (2)$$

$V_c$  is the clearance volume of the cylinder.  $B$ ,  $l$ , and  $r$ , are the cylinder bore, connecting rod's length, and crank radius of the engine, respectively. Moreover,  $s$  is the distance between the piston pin axis and crankshaft axis which is achieved by Eq. (3) [29].

$$s = r \cos \theta + (l^2 + r^2 \sin^2 \theta)^{1/2} \quad (3)$$

### 2.2. Combustion Model

In order to simulate combustion process in the spark ignition engine, Wiebe function is applied which is given in Eq. (4).

$$x_b = 1 - \exp \left[ -a \left( \frac{\theta - \theta_0}{\Delta \theta} \right)^{m+1} \right] \quad (4)$$

where  $\theta$ ,  $\theta_0$ , and  $\Delta \theta$  are crank angle, start of the combustion, and total combustion duration, respectively. The variation of  $x_b$  is from 0 to 0.99. In order to achieve the greater accuracy of simulation, parameters of  $a$  and  $m$  are adjusted with engine operation conditions [30].

### 2.3. The Model of Heat Transfer

The correlation of Woschni is considered for determination of the heat transfer rate through cylinder walls of the engine.

$$h = 0.01298 B^{-0.2} P^{0.8} T^{-0.55} \omega^{0.8} \quad (5)$$

The parameter of  $\omega$  as the average gas velocity in cylinder which is computed by Eq. (6). The coefficients of  $C_1$  and  $C_2$  depend on swirling of in-cylinder gases and engine speed [29].

$$\omega = \left[ C_1 \bar{S}_p + C_2 \frac{V_d T_r}{P_r V_r} (P - P_m) \right] \quad (6)$$

Therefore,  $\frac{dq_w}{d\theta}$  can be achieved via Eq. (7). The simulated model is validated in previous studies [2, 31, 32].

$$\frac{dq_w}{d\theta} = \frac{h \times A_w \times (T_g - T_w)}{6N} \quad (7)$$

### 3. Results and Discussion

#### 3.1. Engine Performance and BSFC

According to introduction section, there are some significant benefits from adding ethanol as a kind of bio-fuel to gasoline. However, it is observed from the general trends of thermal efficiency that ethanol can decrease the percentage of thermal efficiency of the engine as given in Figure 1. Nevertheless, adding hydrogen to this fuel mixture can solve the problem and boost the thermal efficiency of the engine even more than initial figure obtained by using pure gasoline.

According to Figure 1, the percentage of thermal efficiency of the engine with all three different fuels, experiences the lowest values while it is working at 1000 rpm engine speed (26.11%, 23.01%, and 27.14% for G100, G75E25, and G50E25H25, respectively). As the engine speed increases, the thermal efficiencies improve until they reach peak at 32.57% for G100, 32.05% for G75E25, and 32.58% for G50E25H25 at 6000, 5000, and 6000 rpm, respectively.

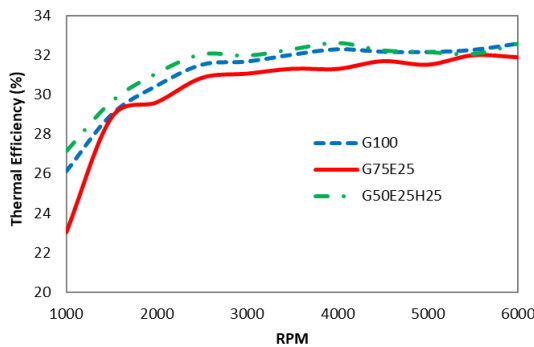


**Figure 1:** Thermal efficiency of the engine using three different fuels vs. engine speed

According to Figure 2, addition of ethanol to pure gasoline increases the amount of brake specific fuel consumption (BSFC) due to the low air-to-fuel ratio of alcoholic fuels. As it is demonstrated in Figure 2, hydrogen addition to ethanol-gasoline blend can control this increment, especially at low engine speeds. This reduction can be explained by the high air-to-fuel ratio of hydrogen fuel and the reduction of the mass flow of total fuel.

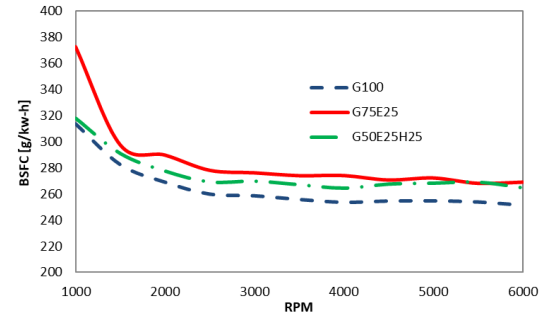


**Figure 2:** BSFC of the engine using three different fuels vs. engine speed

#### 3.2. Combustion Chamber Temperature and Emissions

The reduction of the temperature of combustion chamber causes lower emissions. The gas temperature in combustion chamber at engine speeds of 2000, 4000, and 6000 rpm is illustrated in Figures 3-5, respectively. From Figures 3-5, it is obvious that the curves for the temperature of combustion chamber using G100 and G75E25 are approximately identical, while hydrogen addition could significantly decrease the temperature during power and exhaust strokes.

As shown in Figure 3, the maximum temperature of the gas in combustion chamber at 2000 rpm for G100, G75E25, and G50E25H25 are 2190.59°C, 2211.09°C, and 1915.57°C, respectively. The temperature of gas in combustion chamber using G100 and G75E25 are quite similar, but 25 percent of hydrogen addition can noticeably decrease the maximum temperature by 12.55% due to its high air to fuel ratio. Moreover, there is a fluctuation in gas temperature during the exhaust stroke.

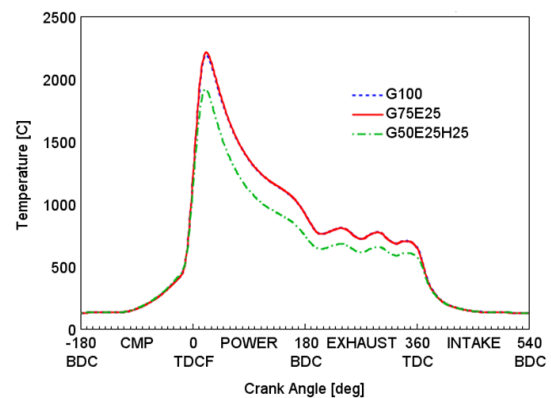


**Figure 3:** Gas temperature in combustion chamber at 2000 rpm

As it is presented in Figure 4, the maximum temperature of the gas in combustion chamber at 4000 rpm for G100, G75E25, and G50E25H25 are 2279.92°C, 2270.98°C, and 2033.17°C, respectively. As it was discussed before, the high air to fuel ratio of hydrogen makes the hydrogen addition an effective technique to decreases the maximum gas temperature in the combustion chamber. Regarding Figure 4, the reduction of maximum gas temperature in the engine using G50E25H25 is 10.82% at 4000 rpm.

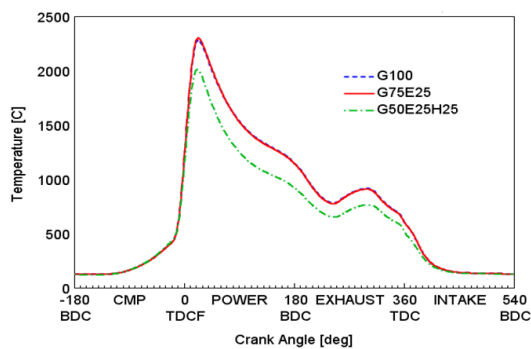


**Figure 4:** Gas temperature in combustion chamber at 4000 rpm

According to Figure 5, the maximum temperature of the gas in combustion chamber at 6000 rpm for G100, G75E25, and G50E25H25 are 2320.87°C, 2346.16°C, and 2009.04°C, respectively. Like the engine operation at 2000 and 4000 rpm, the maximum gas temperature in combustion chamber in the engine using G100 and G75E25 are remarkably similar at 6000 rpm. Addition of hydrogen to the blend reduces the highest temperature of in-cylinder gas by 13.43%.

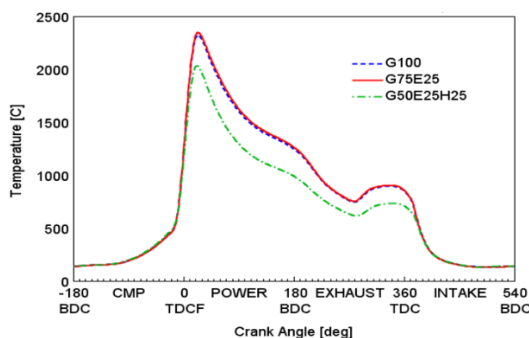


**Figure 5:** Gas temperature in combustion chamber at 6000 rpm

Brake specific carbon dioxide (BSCO<sub>2</sub>) is another significant criterion in aspect of emission production. Adding alcoholic fuels such as ethanol can decrease the amount of

BSCO<sub>2</sub>. As shown in Figure 6, the BSCO<sub>2</sub> of G75E25 is lower than pure gasoline. Furthermore, hydrogen addition would give us the opportunity to emit much lower amount of carbon dioxide as a greenhouse gas (GHG). Regarding Figure 6, the maximum brake specific carbon dioxide for G100, G75E25, and G50E25H25 are 984.671, 993.89, and 946.764 g/kWh, respectively. These values decrease as the engine speed increases and reach 792.151, 769.479, and 771.79 g/kWh at 6000 rpm. The fluctuations of Figure 6 show that the lowest amount of BSCO<sub>2</sub> is related to G50E25H25 fuel blend in most of the engine speeds. The bio-fuel of G75E25 and conventional gasoline are placed in next positions, respectively.

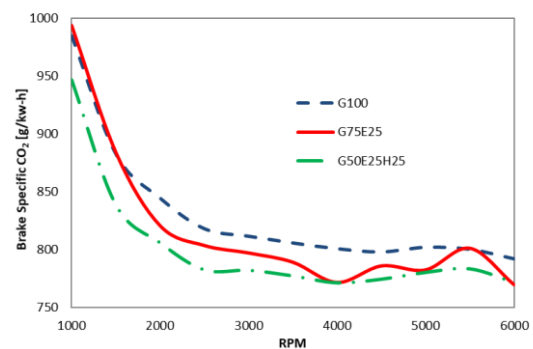


**Figure 6:** BSCO<sub>2</sub> of the engine using three different fuels vs. engine speed

#### 4. Conclusion

In this research, a single-cylinder, four-stroke, and SI engine is investigated numerically in order to simulate the operation conditions of the engine using three different types of fuels including G100, G75E25, and G50E25H25. The following results can be concluded:

- While there are a wide array of benefits by using alcoholic fuels in SI engines which are mentioned in introduction section, addition of ethanol decreases the thermal efficiency of the engine. However, addition of hydrogen by 25% can address this problem and increase the engine thermal efficiency. The comparison between three studied fuels demonstrates that the highest percentage of thermal efficiency is related to the engine using G50E25H25.
- The increment of BSFC is another problem of alcoholic fuels. Nonetheless, this problem is also moderated by hydrogen addition method. It should be

noted that the lowest amount of BSFC is still belongs to G100. G50E25H25 and G75E25 are placed in next orders, respectively.

- The reduction of the temperature of combustion chamber causes lower emissions. The hydrogen-addition technique decreases the maximum gas temperature due to the high air to fuel ratio of hydrogen. In this study, after hydrogen utilization, the maximum temperature of in-cylinder gas decreased by 12.55%, 10.82%, and 13.43% at 2000, 4000, and 6000 rpm, respectively.
- Brake specific carbon dioxide (BSCO<sub>2</sub>) is a prominent parameter in aspect of greenhouse gas emission. The hydrogen-addition method reduces the amount of BSCO<sub>2</sub>. The lowest amount of BSCO<sub>2</sub> is related to G50E25H25 in most of the engine speeds. The bio-fuel of G75E25 and G100 are placed in next positions, respectively.

### List of symbols

$A_w$	Cylinder wall area
$a$	Adjustable parameter
$B$	Cylinder bore
$C_1$	Constant parameter
$C_2$	Constant parameter
$h$	Heat transfer coefficient
$l$	Connecting rod's length
$m$	Adjustable parameter
$N$	Engine speed
$P$	In-cylinder pressure
$P_m$	Motored cylinder pressure
$P_r$	Working-fluid pressure
$q_{in}$	Total heat addition
$q_w$	Heat transfer from the combustion chamber wall
$r$	Crank radius
$s$	Distance between piston pin axis and crank axis
$\bar{S}_p$	Mean piston speed
$T$	Temperature
$T_w$	Wall temperature
$T_g$	In-cylinder gas temperature

$T_r$	Working-fluid temperature
$V$	In-cylinder volume
$V_C$	Cylinder clearance volume
$V_r$	Working-fluid volume
$x_b$	Mass fraction burned

### Greek symbols

$\theta$	Crank angle
$\theta_0$	Start of combustion angle
$\Delta\theta$	Total combustion duration angle
$\gamma$	Specific heat ratio
$\omega$	Average cylinder gas velocity

### References

- [1] Shojaeefard, M., P. Azarikhah, and A. Qasemian, Experimental Investigation of Thermal Balance and Valve Cover Heat Transfer in a Small Internal Combustion Engine. *International Journal of Automotive Engineering*, 2017. **7**(2): p. 2423-2433.
- [2] Qasemian, A., P. Azarikhah, and S. Jenabi Haqparast, Derivation of Specific Heat Rejection Correlation in an SI Engine; Experimental and Numerical Study. *International Journal of Automotive Engineering*, 2018. **8**(2): p. 2679-2691.
- [3] Martins, F., C. Felgueiras, and M. Smitková, Fossil fuel energy consumption in European countries. *Energy Procedia*, 2018. **153**: p. 107-111.
- [4] Braungardt, S., J. van den Bergh, and T. Dunlop, Fossil fuel divestment and climate change: Reviewing contested arguments. *Energy Research & Social Science*, 2019. **50**: p. 191-200.
- [5] Healy, N., J.C. Stephens, and S.A. Malin, Embodied energy injustices: unveiling and politicizing the transboundary harms of fossil fuel extractivism and fossil fuel supply chains. *Energy Research & Social Science*, 2019. **48**: p. 219-234.
- [6] Jenabi Haqparast, S., G.R. Molaeimanesh, and S.M. Mousavi-Khoshdel, Role of phase change materials in creating uniform surface

temperature on a lithium battery cell applicable in electric vehicles. *International Journal of Automotive Engineering*, 2018. **8**(4): p. 2848-2853.

[7] He, H., N. Zhou, J. Guo, Z. Zhang, B. Lu, and C. Sun, Tolerance analysis of electrified vehicles on the motor demagnetization fault: From an energy perspective. *Applied Energy*, 2018. **227**: p. 239-248.

[8] Hovgard, M., O. Jonsson, N. Murgovski, M. Sanfridson, and J. Fredriksson, Cooperative energy management of electrified vehicles on hilly roads. *Control Engineering Practice*, 2018. **73**: p. 66-78.

[9] Björnsson, L.-H. and S. Karlsson, Electrification of the two-car household: PHEV or BEV? *Transportation Research Part C: Emerging Technologies*, 2017. **85**: p. 363-376.

[10] Weiss, M., A. Zerfass, and E. Helmers, Fully electric and plug-in hybrid cars-An analysis of learning rates, user costs, and costs for mitigating CO<sub>2</sub> and air pollutant emissions. *Journal of Cleaner Production*, 2019. **212**: p. 1478-1489.

[11] Dhinesh, B. and M. Annamalai, A study on performance, combustion and emission behaviour of diesel engine powered by novel nano nerium oleander biofuel. *Journal of Cleaner Production*, 2018.

[12] Rigotte, M.R., D. Secco, H.A. Rosa, S.N.M. de Souza, R.F. Santos, F. Gurgacz, and T.R.B. da Silva, Energy efficiency of engine-generator set using biofuels under varied loads. *Renewable and Sustainable Energy Reviews*, 2017. **79**: p. 520-524.

[13] Tompkins, B., H. Song, J. Bittle, and T. Jacobs, Efficiency considerations for the use of blended biofuel in diesel engines. *Applied Energy*, 2012. **98**: p. 209-218.

[14] Ospina, G., M.Y. Selim, S.A. Al Omari, M.I.H. Ali, and A.M. Hussien, Engine roughness and exhaust emissions of a diesel engine fueled with three biofuels. *Renewable Energy*, 2018.

[15] Szabados, G., Á. Bereczky, T. Ajtai, and Z. Bozóki, Evaluation analysis of particulate

relevant emission of a diesel engine running on fossil diesel and different biofuels. *Energy*, 2018. **161**: p. 1139-1153.

[16] Masera, K. and A. Hossain, Biofuels and thermal barrier: A review on compression ignition engine performance, combustion and exhaust gas emission. *Journal of the Energy Institute*, 2018.

[17] Wei, H., D. Feng, M. Pan, J. Pan, X. Rao, and D. Gao, Experimental investigation on the knocking combustion characteristics of n-butanol gasoline blends in a DISI engine. *Applied Energy*, 2016. **175**: p. 346-355.

[18] Rothamer, D.A. and J.H. Jennings, Study of the knocking propensity of 2, 5-dimethylfuran-gasoline and ethanol-gasoline blends. *Fuel*, 2012. **98**: p. 203-212.

[19] Wei, H., D. Feng, J. Pan, A. Shao, and M. Pan, Knock characteristics of SI engine fueled with n-butanol in combination with different EGR rate. *Energy*, 2017. **118**: p. 190-196.

[20] Mack, J.H., V.H. Rapp, M. Broeckelmann, T.S. Lee, and R.W. Dibble, Investigation of biofuels from microorganism metabolism for use as anti-knock additives. *Fuel*, 2014. **117**: p. 939-943.

[21] Hamid, M., M. Idroas, S. Sa'ad, A.S. Bahri, C. Sharzali, M. Abdullah, and Z. Zainal, Numerical investigation of in-cylinder air flow characteristic improvement for Emulsified biofuel (EB) application. *Renewable Energy*, 2018. **127**: p. 84-93.

[22] Mane, S.D., Experimental Investigation of Single Cylinder Direct Injection CI Engine Performance Using Biofuels. *Materials Today: Proceedings*, 2018. **5**(11): p. 22901-22907.

[23] Azoumah, Y., J. Blin, and T. Daho, Exergy efficiency applied for the performance optimization of a direct injection compression ignition (CI) engine using biofuels. *Renewable Energy*, 2009. **34**(6): p. 1494-1500.

[24] Jeevahan, J., R.D. Sriramanjaneyulu, and G. Mageshwaran, Experimental Investigation of the suitability of 1-Butanol Blended with Biodiesel as an Alternative Biofuel in Diesel

Engines. Biocatalysis and Agricultural Biotechnology, 2018.

[25] Gupta, S.K. and M. Mittal, Effect of Compression Ratio on the Performance and Emission Characteristics, and Cycle-to-Cycle Combustion variations of a Spark-Ignition Engine Fueled with Bio-methane Surrogate. Applied Thermal Engineering, 2019. **148**: p. 1440-1453.

[26] Nayyar, A., D. Sharma, S.L. Soni, B. Bhardwaj, and M. Augustine, Modeling and experimental investigation for performance and emissions on a diesel engine using bio-oxygenated ternary fuel blends. Energy, 2019. **168**: p. 136-150.

[27] Galloni, E., F. Scala, and G. Fontana, Influence of fuel bio-alcohol content on the performance of a turbo-charged, PFI, spark-ignition engine. Energy, 2019. **170**: p. 85-92.

[28] Natarajan, S. and A.M. Sundareswaran, Computational analysis of an Early Direct Injected HCCI engine using Bio ethanol and Diesel Blends as Fuel. Energy Procedia, 2017. **105**: p. 350-357.

[29] Heywood, J.B., Internal combustion engine fundamentals. Vol. 930. 1988: McGraw-hill New York.

[30] Ferguson, C.R. and A.T. Kirkpatrick, Internal combustion engines: applied thermosciences. Third ed. 2016: John Wiley & Sons.

[31] Azarikhah, P., S.J. Haghparast, and A. Qasemian, Investigation on total and instantaneous energy balance of bio-alternative fuels on an SI internal combustion engine. Journal of Thermal Analysis and Calorimetry, 2019.

[32] Qasemian, A., S.J. Haghparast, P. Azarikhah, and M. Babaie, Effects of compression ratio of bio-fueled SI engines on the thermal balance and waste heat recovery potential. Sustainability, 2021. **13**(11): p. 5921.